Neurocomputing 74 (2011) 3502–3508

Contents lists available at ScienceDirect

Neurocomputing

journal homepage: www.elsevier.com/locate/neucom

The neural dynamics for hysteresis in visual perception

Hongzhi You, Yan Meng, Di Huan, Da-Hui Wang *

Department of Systems Science, Beijing Normal University, Beijing 100875, China

ARTICLE INFO

Article history:
Received 3 October 2010
Received in revised form
4 June 2011
Accepted 6 June 2011
Communicated by I. Bojak
Available online 25 June 2011

Keywords:
Hysteresis
Spiking neuron network
Slow dynamic system
Multiple steady states
Swallowtail catastrophe

ABSTRACT

The hysteresis in the perception has been observed in many perceptual experiments, but little is known about the underlying dynamical mechanism. We simulate a visual discrimination task, as an example of hysteresis in the perception, using a spiking neuron network and the corresponding slow dynamic system. The hysteresis in visual perception has been reproduced in our simulation. We find that hysteresis is influenced by the change speed of the external stimuli and the excitatory recurrent interaction inside the selective neuron pool. The slow dynamic system reveals the dynamical mechanism underlying the hysteresis: emerging from the lag between the response of neural system and the fast change external stimuli when the slow dynamic system has a single steady state; emerging from the multiple steady states regardless of the change speed of the external stimuli. In particularly, the multiplicity of the steady state of the slow dynamic system comes from the codimension three swallowtail catastrophe which exhibits two interacting cusp catastrophes.

1. Introduction

The hysteresis in the perception means that what is perceived depends on previous experiences. Hysteresis is a typical phenomenon in visual, auditory, and somatosensory perceptions and has been extensively observed for many perceptual tasks [1–6]. An example of this phenomenon is a motion perception task in which some dots were moving in random directions, while other dots were moving coherently in a vertical direction on the screen. The coherence level gradually increased at first and then gradually decreased. The subjects could perceive the vertical motion at a threshold of the coherence level and note the disappearance of the vertical motion at another threshold. The experiment showed that the former threshold was larger than the latter threshold, which implied that the perception of the vertical motion depends on the history of the stimuli presentation [1]. In another experiment [2], the subjects were required to detect a hidden letter on the screen whose contrast gradually increased at first and then gradually decreased. The subjects were aware of the letter at one threshold when the contrast was increased. However, the subjects noted the disappearance of the letter at another threshold when the contrast was decreased. This experiment showed that the threshold of the increasing contrast was larger than that of the decreasing contrast. At the same time, the magnetic resonance signal also demonstrated the hysteresis phenomenon [2]. For an auditory system, the threshold to detect a tone whose amplitude increased was higher than the threshold for a tone that became inaudible. A recent study about the mosquito's auditory system showed the hysteresis of the antennal response to a sound with a single frequency [6].

Hysteresis in the perception has been observed for a long time, but little is known about the underlying neural mechanism, especially how hysteresis can emerge from single neuron activities. Hirai and Fukushima proposed a multiple layer model to investigate the binocular parallax, and their model exhibited hysteresis in binocular depth perception as observed by Fender and Jules but without explanation of the key factors that induced hysteresis [21,22]. Recently, Wilson and his coworkers proposed that positive feedback and recurrent inhibition between neural units could cause hysteresis [23]. A more quantitative explanation is that cusp catastrophe or bistability underlies the hysteresis in the perception [3,4,7]. Actually, a cusp catastrophe system has two stable steady states and the back-and-forth transition pathway between two stable steady states depending on the increase or decrease of the control parameter. However, the cusp catastrophe is only an analogous explanation of hysteresis in the perception, and the relationship between the microscopic neural activities and the hysteresis in the perception for macroscopic behavior has not yet been established. Therefore, we apply a network with spiking neurons to simulate a simple visual discrimination task and the neural activities are demonstrated as an example of hysteresis in the perception. At the same time, we derive a two-variable slow dynamic system from the spiking neuron network. By analyzing the steady states of the slow dynamic system, we find that the slow dynamic system can operate under different regimes and the multiple stable states

* Corresponding author. Tel.: +86 10 58807876.
E-mail address: wangdh@bnu.edu.cn (D.-H. Wang).

0925-2312/$ - see front matter © 2011 Elsevier B.V. All rights reserved.
doi:10.1016/j.neucom.2011.06.004

lead to hysteresis in the perception. We also find that stronger recurrent excitation and faster change of the external stimuli both favor hysteresis.

2. The spiking neuron model and the slow dynamic system

To investigate the neural dynamics underlying hysteresis in the perception, we start from a comparable simple task described in [3–5,7]. In this visual perception experiment, the subjects have to observe a series of figures one after another and to discriminate those in which the visual stimuli gradually change from a man's face to a kneeling girl (Fig. 1). Subjects notice the jump from the man's face to the kneeling girl at one point when subjects watch the figures from left to right. The same observation in the reverse direction, from right to left, shows that the transition from the kneeling girl to the man's face occurs at a later point. In this task, the perception of the man's face or the kneeling girl is a kind of choice between the man's face and the kneeling girl, so we adopt a spiking neuron network for a two-alternative choice to simulate the task [9].

The spiking neuron model [9,10] is composed of N neurons, with N_E pyramidal cells (80%) and N_I interneurons (20%). The pyramidal cells are subdivided into one nonselective neuron pool and two selective neuron pools, I and II, which prefers the man's face and the kneeling girl, respectively. One of the selective pools receives the stimuli denoting the man's face and the other receives the stimuli representing the kneeling girl. Each selective pool has fN_E pyramidal cells, and here we choose $N_E=1600$ and $f=0.15$. The architecture of the model is an all-to-all network with pyramid-to-pyramid, pyramid-to-interneuron, interneuron-to-pyramid, and interneuron-to-interneuron connections. Fast AMPA receptors and slow NMDA receptors mediate the recurrent excitatory postsynaptic currents (EPSCs), and GABA receptors mediate the recurrent inhibitory postsynaptic currents (IPSCs). External EPSCs including the stimuli and background noise are mediated exclusively by AMPA receptors. We use w_+ to denote the relative connection strength inside the selective pool, and w_- to denote the relative connection strength between the selective pools and those from the nonselective to the selective pool. Other relative connection strengths equal one. To keep the overall recurrent excitation constant in the spontaneous state when w_+ is varied, we choose $w_-=1-f(w_+-1)/(1-f)$ [11].

We chose the leaky integrate-and-fire model to depict the dynamics of both pyramidal cells and interneurons [12], which are characterized by a resting potential $v_L=-70$ mV, a firing threshold $v_{th}=-50$ mV and a reset potential $v_{reset}=-55$ mV. The subthreshold membrane potential $v(t)$ follows the first-order equation:

$$C_m\frac{dv(t)}{dt}=-g_L(v(t)-v_L)-I_{syn}(t) \tag{1}$$

where the membrane capacitance C_m is 0.5 nF for pyramidal cells and 0.2 nF for interneurons. The leak conductance g_L is 25 nS for pyramidal cells and 20 nS for interneurons, and the refractory period τ_{ref} is 2 ms for pyramidal cells and 1 ms for interneurons. $I_{syn}(t)$ is the total synaptic current input to the neuron and is given as follows:

$$I_{syn}(t)=I^A_{ext}(t)+I^A_{rec}(t)+I^N_{rec}(t)+I^G_{rec}(t)$$

$$I^A_{ext}(t)=g^A_{ext}(v(t)-v_E)s^A_{ext}(t)$$

$$I^A_{rec}(t)=g^A_{rec}(v(t)-v_E)\sum_{j=1}^{N_E}w_j s^A_j(t)$$

$$I^N_{rec}(t)=\frac{g^N_{rec}(v(t)-v_E)}{(1+[\mathrm{Mg}^{2+}]e^{-0.062v(t)/3.57})}\sum_{j=1}^{N_E}w_j s^N_j(t)$$

$$I^G_{rec}(t)=g^G_{rec}(v(t)-v_I)\sum_{j=1}^{N_I}w_j s^G_j(t)$$

where $v_E=0$ mV, $v_I=-70$ mV, $[\mathrm{Mg}^{2+}]=1$ mM [13]. The symbols A, N and G denote AMPA, NMDA and GABA receptors, respectively. We use the following values for the synaptic conductances (in nS) in the spiking neuron network [9]: for pyramidal cells, $g^A_{ext}=2.1$, $g^A_{rec}=0.05$, $g^N_{rec}=0.165$, and $g^G_{rec}=1.3$; for interneurons, $g^A_{ext}=1.62$, $g^A_{rec}=0.04$, $g^N_{rec}=0.13$, and $g^G_{rec}=1.0$. The gating variable s for AMPA and GABA obeys the first-order dynamics:

$$\frac{ds^A_j}{dt}=-\frac{s^A_j}{\tau^A}+\sum^k\delta(t-t^k_j) \tag{2}$$

$$\frac{ds^G_j}{dt}=-\frac{s^G_j}{\tau^G}+\sum^k\delta(t-t^k_j) \tag{3}$$

where $\tau_A=2$ ms and $\tau_G=5$ ms [14–16]. $\delta(t-t^k_j)$ denotes the spike train of presynaptic neurons. The gating variable s for NMDA follows the first-order dynamics:

$$\frac{ds^N_j}{dt}=-\frac{s^N_j}{\tau^N_{decay}}+\alpha x_j(1-s^N_j) \tag{4}$$

$$\frac{dx_j}{dt}=-\frac{x_j}{\tau^N_{rise}}+\sum^k\delta(t-t^k_j) \tag{5}$$

where $\tau^N_{decay}=100$ ms, $\tau^N_{rise}=2$ ms and $\alpha=0.5$ ms^{-1} [14,15]. Note that all synapses have a latency of 0.5 ms.

Because each figure consists of the features of the man's face and kneeling girl, the stimuli of each figure to the spiking neuron model could be described as two independent Poisson spike trains, one for the man's face to neuron pool I and the other for the kneeling girl to neuron pool II. The feature of the man's face will decrease and the feature of the kneeling girl will increase when the figures morph from the man's face into the kneeling girl. Therefore, the frequency of the spike train to neuron pool I will decrease and the frequency of spike train to neuron pool II will increase when the figure changes from the man's face to the kneeling girl as shown in Fig. 2(a)(bottom): $r_m(t)=60(1-t/T)$ Hz for the man's face, and $r_g(t)=60t/T$ Hz for the kneeling girl, where t is the simulation time, and the subjects take time T to finish one trial of observation from left to right or from right to left in Fig. 1. The stimuli can be rewritten as $r_m=30-30\phi$ Hz and $r_g=30+30\phi$ Hz with $\phi\in[-1,1]$. The increase of ϕ denotes the fading out of the man's face and the emergence of the kneeling girl, while the decrease of ϕ denotes the reverse direction of the stimuli presentation. For external AMPA mediated currents, the background Poisson spike trains are independent from cell to cell and the spike trains have same frequency $v_{ext}=2.4$ kHz.

In the spiking neuron model, the gating variables of NMDA receptors are much slower than other variables. The typical behavior of the system could be captured by those slow variables according to the slaving principal [7] or adiabatic elimination [8]. Therefore, the spiking neuron model can be simplified into a

Fig. 1. The figures from left to right morph from a man's face to a kneeling girl, which is adapted from [5,7].

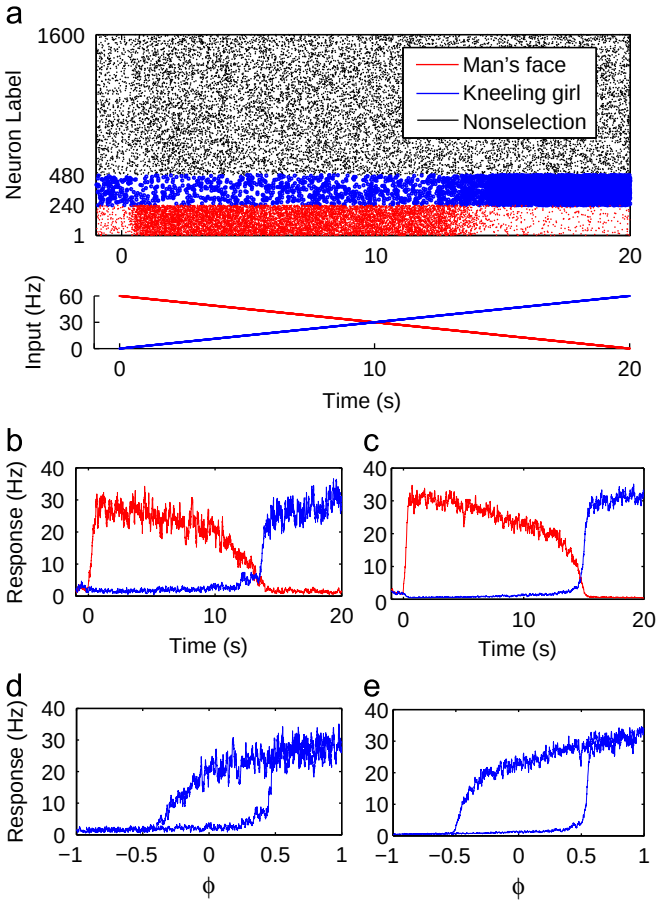

Fig. 2. The example of the time evolution of the spiking neuron network and the slow dynamics. (a) The raster plot of the neural activity in spiking neuron network (top) and the simulation protocol (bottom). (b) The population firing rate of two selective neuron pools. (c) The time course of firing rate transferred from the slow dynamics using the relation: $r_i = H(x_i)$ [17]. (d) The activity of the kneeling girl selective neuron pool exhibits hysteresis. (e) The slow dynamics for the kneeling girl also demonstrates hysteresis.

nonlinear dynamic system with two variables related with NMDA gating variables (the details of the derivation can be found in [17]):

$$\frac{dS_1}{dt} = f_1(S_1,S_2) = -\frac{S_1}{\tau_S} + (1-S_1)\gamma H(x_1) \tag{6}$$

$$\frac{dS_2}{dt} = f_2(S_1,S_2) = -\frac{S_2}{\tau_S} + (1-S_2)\gamma H(x_2) \tag{7}$$

where $S_1 (\in [0,1])$ for pool I, $S_2 (\in [0,1])$ for pool II, $H(x_i)$ is the input–output relation, $H(x_i) = (ax_i - b)/(1-\exp(-d(ax_i-b)))$, $x_1 = J_{N,11}S_1 - J_{N,12}S_2 + I_0 + I_1 + I_{noise,1}$, $x_2 = J_{N,22}S_2 - J_{N,21}S_1 + I_0 + I_2 + I_{noise,2}$, $J_{N,11} = J_{N,22} = 0.3893w_+ - 0.4009$, and $J_{N,12} = J_{N,21} = 0.0687w_+ - 0.0571$. The kinetic parameters are $\tau_S = 100$ ms and $\gamma = 0.641$. Parameters for the input–output function are $a = 270$ (VnC)$^{-1}$, $b = 108$ Hz, and $d = 0.154$ s. The overall effective external input to each pool is $I_0 = 0.3255$ nA. The stimuli of one figure is described as $I_1 = J_{A,ext}r_m$ to neuron pool I, and $I_2 = J_{A,ext}r_g$ to neuron pool II, where $J_{A,ext} = 5.2 \times 10^{-4}$ nA Hz^{-1} is the average synaptic coupling with AMPARs. The background noise is an Ornstein–Uhlenbeck process:

$$\tau_A \frac{dI_{noise,i}}{dt} = -I_{noise,i} + \eta(t)\sqrt{\tau_A \sigma^2_{noise,i}} \tag{8}$$

where $i = 1,2$ and $\eta(t)$ is a white noise with $\langle \eta(t)\eta(t')\rangle = \sigma^2_{noise}\delta(t-t')$. The noise amplitude is $\sigma_{noise} = 0.02$ nA. The slow dynamic system (6)–(8) has been used to reveal the mechanism underlying two-alternative decision making and the parameters have been calibrated in [17]. In this paper, we apply the nonlinear analysis method to the slow dynamic system and investigate how hysteresis can emerge from the neural activity.

3. Hysteresis of the neural activity

Assuming that subjects take 20 s ($T = 20$ s) to finish one trial of observation from left to right, the frequency of the Poisson spike train to the neuron pool I decreases from 60 to 0 Hz and that to the neuron pool II increases from 0 to 60 Hz in the simulation (the bottom panel of Fig. 2(a)). The raster plot, shown in the upper panel of Fig. 2(a), indicates that the activity of the nonselective neuron pool is almost invariant to the changing inputs. However, the activity of the man's face selective neuron pool I gradually decreases and that of the kneeling girl selective neuron pool II gradually increases with the changing input. The population firing rates of two selective neuron pools are shown in Fig. 2(b). One notable thing here is that the crossover of the two population firing rates, about 14 s and $\phi = 0.4$, is behind the crossover of the frequency of two input spike trains (at 10 s). Considering the rule of the winner-take-all mechanism in many neural systems, we assume that the network perceives the man's face if the neurons in the pool I fire more spikes than that in the pool II, and vice versa. Therefore, in the simulation trial shown in Fig. 2(a) and (b), the jump from the man's face to the kneeling girl or perception switching occurs at time 14 s or parameter $\phi = 0.4$.

Besides the observation from left to right, we also simulate the trial of observation from right to left. In the reverse direction trial, the initial stimuli of the man's face is smaller than that of the kneeling girl. The population firing rate of the neuron pool I increases and that of the neuron pool II decreases along with the decrease of ϕ. The perception switches at another point $\phi = -0.4$. In Fig. 2(d), we plot the population firing rate of the neuron pool II for two different directions of observation over the parameter (ϕ). The plots show a typical hysteresis loop of neural activity. At the same time, the activity of the neuron pool I also demonstrates a typical hysteresis loop but the data are not shown. Because the activities of two selective neuron pools have hysteresis loops and their cross points are different given increasing or decreasing ϕ, the switching point of perception (SPP) given increasing ϕ differs SPP given decreasing ϕ.

The slow dynamic system is simplified from the spiking neuron model; thus, it should demonstrate similar hysteresis. We calculated the slow dynamic system (6)–(8) using a fourth order Runge–Kutta algorithm given the same inputs as those of the spiking neuron model. The response to the man's face decreases while the response to the kneeling girl increases as shown in Fig. 2(c), in which the perception switches later than the stimuli. The response for the kneeling girl shows a hysteresis loop in Fig. 2(e). Thus, the spiking neuron model and the corresponding slow dynamic system demonstrate hysteresis phenomenon similar to the hysteresis observed in experiments.

4. The effects of asymptotic and transient behavior of neural networks on hysteresis

The hysteresis of neural activity in this visual perception task have been demonstrated in Section 3. In this section, we will investigate the factors that influence hysteresis. Generally speaking, the dynamics of the neuron network, including asymptotic and transient behavior, have important impacts on neural activity. As for the asymptotic behavior, the relative connection

strength inside the selective neuron pools w_+ plays a significant role. The bigger w_+ results in a stronger recurrent excitation inside the selective pool and a weaker competition between selective pools, which favors the persistent activity in one selective neuron pool [18,19]. The persistent activity means that the network memorizes the input information, which could result in hysteresis.

To investigate the effect of asymptotic behavior on hysteresis, we vary the relative connection strength w_+, which determines the asymptotic behavior of the system. We simulate the spiking neuron model and the slow dynamic system with fixed $T(=20\ \mathrm{s})$ and different w_+. As shown in Fig. 3(a), the hysteresis loop is almost vanishing given $w_+=1.55$, while it becomes significant given $w_+=1.65$, which indicates that the increase of w_+ enlarges the hysteresis loop. The consequence of the larger hysteresis loop is a larger delay between the perception switching and the stimuli switching. The results in Fig. 3(e) show that the increase of w_+ monotonically prolongs the delay between the switching point of the perception and the switching point of the stimuli given the fixed T, which is consistent with the consequence of an enlarging hysteresis loop. We obtain the same results as that of the slow dynamics as shown in Fig. 3(b) and (f). These results indicate that the stronger excitation inside the selective pools favors hysteresis in the perception.

For the transient behavior, the response time constant of the neuron network determines the speed of its response to the external stimuli. The slow response cannot keep pace with the fast change of the external stimuli. Additionally, the network may overshot because of recurrent excitation, which leads to the difference of the switching point of perception and that of the stimuli. To test this hypothesis, we set all parameters of the neural network as constants, which implies that the response time constant of the neural network is fixed. We change the duration of the stimuli presentation T and fix the variation range of the stimuli. A longer T means slower change of the external stimuli while a shorter T means faster change of the external stimuli. We show the activity of the neuron pool preferring the kneeling girl given the same $w_+(=1.65)$ and different T in Fig. 3(c). The results indicate that a faster change of external stimuli leads to a larger hysteresis loop and a slower change of external stimuli induces a smaller hysteresis loop. This result is consistent with a recent psychophysical research about the hysteresis in stereopsis and binocular rivalry [23]. In the experiment, a shorter frame duration of the movie sequence leads to a larger hysteresis loop (see Fig. 2 in [23]).

To quantify the overall effects of change speed of the external stimuli and the relative connection strength on hysteresis, we show the SPP given different change speeds of external stimuli and different recurrent connection strengths. The results, shown in Fig. 3(e), indicate that a faster change of external stimuli and a stronger connection strength lead to a larger SPP and more significant hysteresis in the perception. The counterpart results of the slow dynamic system are shown in Fig. 3(b), (d), and (f).

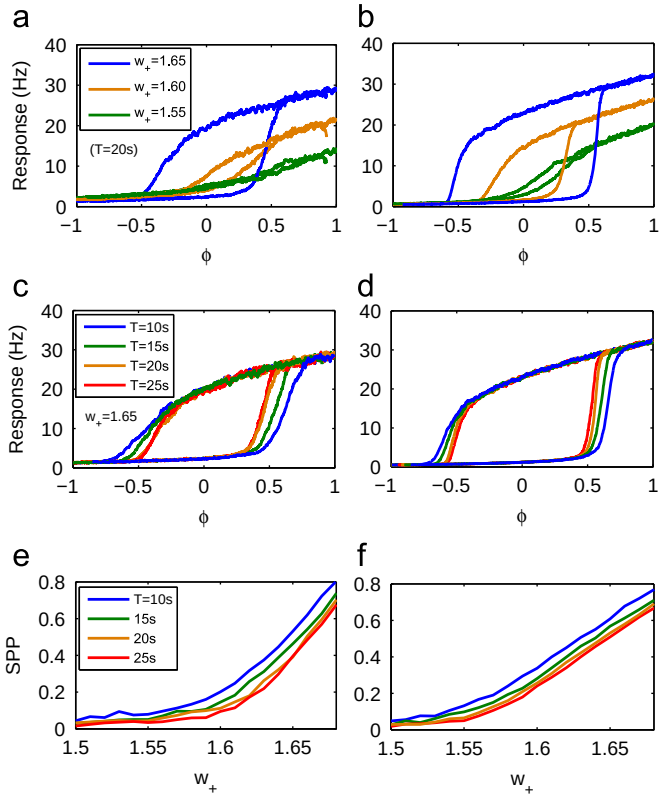

Fig. 3. The effects of w_+ and T on the hysteresis in the perception. The responses for the kneeling girl with different w_+ are shown in (a) for the spiking neuron network, and in (b) for the slow dynamics, respectively. The results indicate that the increase of w_+ enlarges the hysteresis loop and enhances the hysteresis. The responses for the kneeling girl with different T are shown in (c) for the spiking neuron network, and in (d) for the slow dynamics. The faster change of external stimuli enlarges the hysteresis loop. The system follows its asymptotic behavior when the change of external stimuli is slow. The switching point of the perception (SPP) with different recurrent strengths w_+ and different T of the spiking neuron network and the slow dynamics are shown in (e) and (f), respectively.

5. Multiple stable steady states lead to hysteresis in the perception

Fig. 3 demonstrates that the increase of the relative excitation in the selective neuron pool or speedup of the external stimuli leads to more obvious hysteresis in the perception. The similarity between the results about the spiking neuron model and the slow dynamic system suggests that we can reveal the neural dynamics of the hysteresis in the perception using nonlinear analysis of the slow dynamic system. By setting the right hand side of Eqs. (6) and (7) as zero, we obtain two algebra equations about S_1 and S_2. The steady state of the slow dynamic system can be obtained by solving these two equations. Assuming that $(\hat{S}_1,\hat{S}_2)$ is a steady state of the slow dynamic system, then the Jacobian matrix of the system about this steady state is

$$J=\left[\begin{array}{cc}\frac{\partial f_1}{\partial S_1} & \frac{\partial f_1}{\partial S_2}\\ \frac{\partial f_2}{\partial S_1} & \frac{\partial f_2}{\partial S_2}\end{array}\right]_{(\hat{S}_1,\hat{S}_2)} \tag{9}$$

where $\partial f_i/\partial S_j=-\delta_{i,j}[1/\tau_s+\gamma H(x_i)|_{(\hat{S}_1,\hat{S}_2)}]+(1-\hat{S}_i)\gamma J_{N,ij}\partial H/\partial x_i|_{(\hat{S}_1,\hat{S}_2)}$, where $\delta_{i,j}=1$ if $i=j$, and $\delta_{i,j}=0$ if $i\neq j$. The sign of the real part of the eigenvalues of the Jacobian matrix at the steady state determines the stability of the steady state. The negative real part of the eigenvalue corresponds to the stable steady state, and the positive real part of the eigenvalue corresponds to the unstable steady state [20].

We first calculate the steady state of the slow dynamic system with a fixed average synaptic coupling with AMPARs ($J_{A,ext}=5.2\times10^{-4}\ \mathrm{nA\,Hz^{-1}}$), the variant recurrent connection inside the selective neuron pool w^+, and the increasing ϕ. The results are shown in Fig. 4. When w^+ is small, the competition between two selective neuron pools is weak. The system has only one stable steady state (Fig. 4(a) and (b)). The asymptotic dynamics of the system does not support the hysteresis because the steady states of $\hat{S}_1$ and $\hat{S}_2$ cross at $\phi=0$. However, the fast change of external stimuli may make the system unable to keep pace with the external stimuli and results in hysteresis. When $1.588<w_+<1.595$, the slow dynamic system has five steady states in the neighborhood of

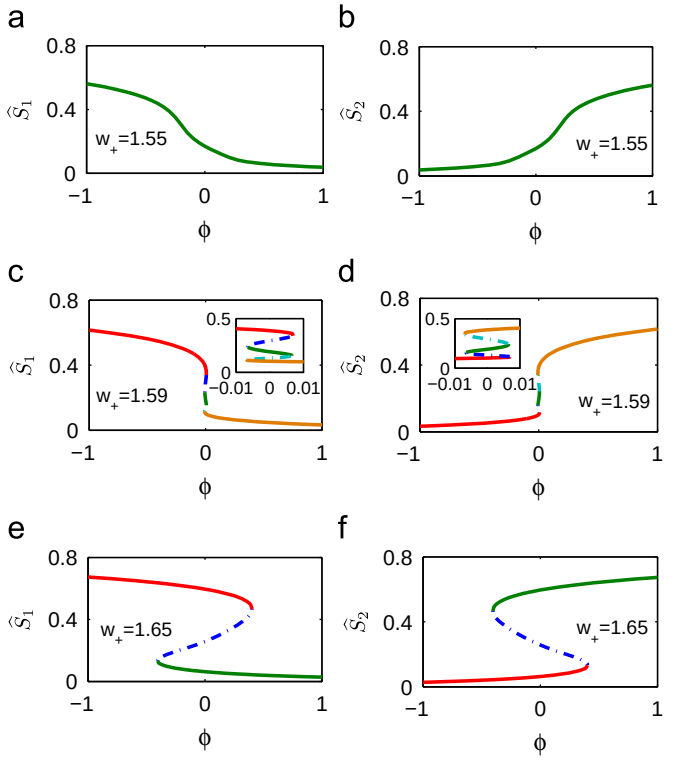

Fig. 4. The steady states of the slow dynamic system. The solid line denotes the stable steady state, and the dash line denotes the unstable steady state. (a,b) The slow dynamic system has only one steady state, where $w_+=1.55$. (c,d) Along with the increase of ϕ, the number of the steady states changes from one to five, and finally to one. The inset figure shows the five steady states. Three of them are stable and the other two are unstable. (e,f) The number of steady states changes from one to three and finally to one. One of three steady states is unstable and locates between two stable states. The S-shape of the steady states leads to the hysteresis.

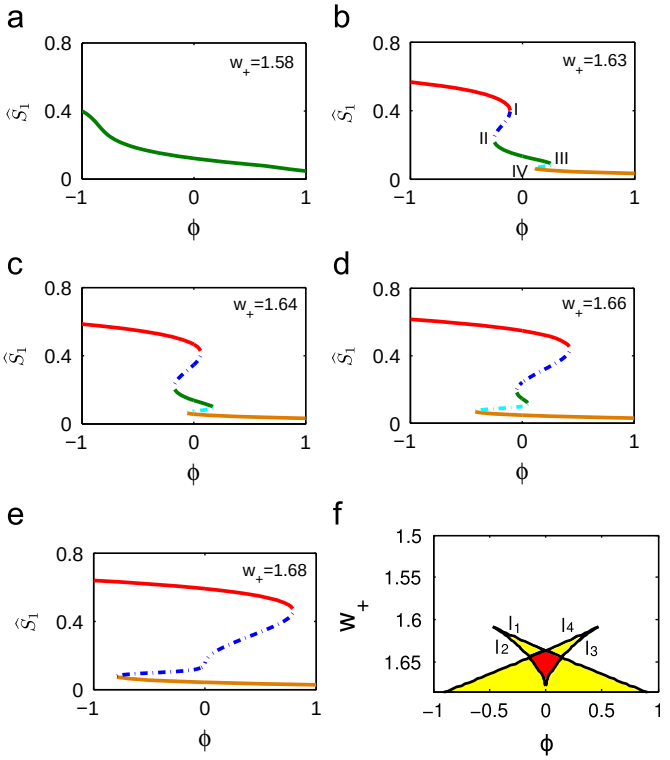

Fig. 5. An example of interaction between two cusps. (a) Small w^+ leads to single steady state. (b) Two cusps emerge with the increase of w^+ and there are four critical steady states I, II, III, and IV. (c,d) The upper cusp develops rightward and the lower cusp develops leftward with the further increase of w^+, in other word, critical steady states I and II increase while the critical steady states III and IV decrease. (e) The critical steady states II and III coalesce and the two cusps finally collapse into one big cusp. (f) The locus of four critical steady states demonstrates two overlapping cusps. Two cusps overlap in red area, in which the slow dynamic system has five steady states. The slow dynamic system has three steady states in the yellow area. (For interpretation of the references to color in this figure legend, the reader is referred to the web version of this article.)

$\phi=0$ (Fig. 4(c) and (d), especially, see the inset of the figures). Three of them are stable, and the other two are unstable. When $w_+>1.595$, the system has strong excitatory recurrent inside the selective pool and the competition between selective pools is strong. Along with the increase of ϕ, the number of steady states of the system changes from one to three and then to one (Fig. 4(e) and (f)). The system has three steady states if $\phi\in[\phi_1,\phi_2]$, where $\phi_1<0$ and $\phi_2>0$. Two of them are stable, and the other is unstable. These three steady states can account for the hysteresis in the perception. When ϕ increases from -1 to 1, the neuron network perceives the man's face until $\phi>\phi_2$. While ϕ decreases from 1 to -1, the neuron network perceives the kneeling girl until $\phi<\phi_1$. Thus, the hysteresis emerges from this multiple-stability of the system.

Notably, there is a small parameter domain supporting five steady states in Fig. 4, which is different from the previous studies [3,4,7]. To clearly demonstrate the bifurcation of the slow dynamic system, we vary other parameters besides w^+ and ϕ. We find that the slow dynamic system is codimension three and the parameters $J_{A,ext}$, w^+, and ϕ control the bifurcation, which exhibits a swallowtail catastrophe caused by two interacting cusps. We show an example of the interaction between two cusps in Fig. 5, where $J_{A,ext}$ is fixed as 2.5×10^{-4} nA Hz^{-1}, w^+ and ϕ are variant. For simplification, only the values of $\hat{S}_1$ are shown. The system has one steady state if w^+ is small (Fig. 5(a)). Along with the increase of w^+, the system has multiple steady states and two separate cusps emerge simultaneously, one locates at upper and the other locates at the lower segment of steady state curve of $\hat{S}_1$. Two cusps include four critical steady states, labeled as I, II, III, and IV from top to bottom in Fig. 5(b). The upper cusp develops rightward and the lower cusp develops leftward with the increase of w^+, in other words, ϕ of the critical steady states I and II increase and ϕ of critical steady states III and IV decrease with the increasing w^+. Once ϕ of the critical steady state I equals and then becomes larger than that of the critical steady state IV, the slow dynamic system has five steady states as shown in Fig. 4(c) and (d), as well as in Fig. 5(c). The further increase of w^+ leads to further leftward shift of the upper cusp and further rightward shift of the lower cusp (Fig. 5(d)). When the critical steady state II meets III, the two cusps collapse into one bigger cusp as shown in Fig. 5(e). The loci of the critical steady states are drawn in Fig. 5(f). The lines l_1, l_2, l_3, and l_4 correspond to the critical steady states I, II, III, and IV, respectively. The lines l_1 and l_2 depict the upper cusp and the lines l_3 and l_4 depict the lower cusp. In the overlapping area of upper and lower cusps, the system has five steady states (red area in Fig. 5(f)).

The overlapping area of two cusps in Fig. 5(f), which is controlled by the parameter $J_{A,ext}$, decreases with the increase of parameter $J_{A,ext}$ and finally vanishes. We show an example that the slow dynamic system has only one cusp with $J_{A,ext}=6.9\times10^{-4}$ nA Hz^{-1} in Fig. 6. The system has a single steady state given small w^+ in Fig. 6(a). The number of steady states varies from one to three then to one along with the increase of ϕ given a large w^+ in Fig. 6(b). The locus of the critical steady state is shown in Fig. 6(c), which is same as the usual cusp [3,4,7]. However, the whole picture of the bifurcation of the slow dynamic system is obviously not a cusp catastrophe with codimension two. As shown in Fig. 6(d), the slow dynamic system is codimension three, and the

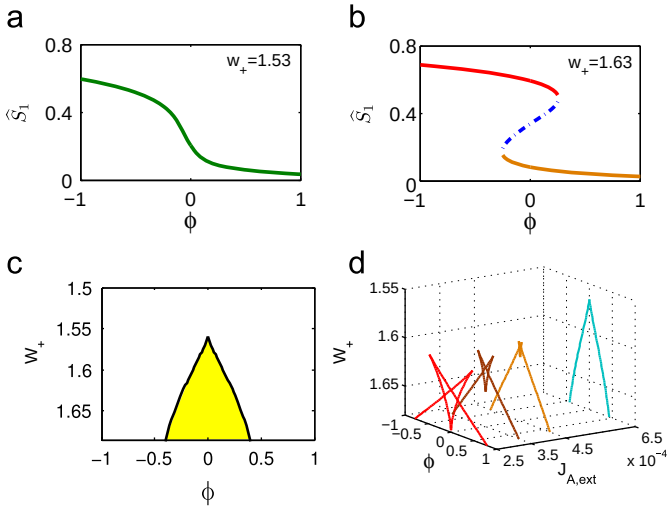

Fig. 6. The overlapping of two cusps controlled by $J_{A,ext}$. (a,b) The slow dynamic system, with a large $J_{A,ext}(=6.9\times10^{-4}$ nA Hz$^{-1})$, has a single steady state given small w^+ and three steady state with large w^+. (c) The loci of the critical steady states, which are the same as the usual cusp. The slow dynamic system has three steady states in the yellow area. (d) The loci of critical steady states given four different $J_{A,ext}$. The overlapping area of two cusps decreases with the increasing $J_{A,ext}$ and two cusps collapse into one big cusp. (For interpretation of the references to color in this figure legend, the reader is referred to the web version of this article.)

parameter $J_{A,ext}$ controls the overlapping of two cusps. With the increasing of $J_{A,ext}$, the overlapping area decreases and finally vanishes when two coexisted cusp becomes one cusp as shown in Fig. 6(d). From the above analysis, we find that the slow dynamic system reveals a codimension three swallowtail catastrophe, which is controlled by three parameters: $J_{A,ext}$, w^+ and ϕ.

6. Conclusion and discussion

In conclusion, we demonstrate the hysteresis in the perception using an example of simple visual discrimination task. By simulation of a spiking neuron network and analysis of the corresponding slow dynamic system, we find two factors affecting the hysteresis of perception: one is the strength of the synapse, the other is the change speed of the external stimuli. The simulation shows that a stronger connection inside the selective neuron pool leads to a larger hysteresis loop of the neuron activities, which results in a larger gap between the two points of the perception switching. The results are consistent with previous results about working memory, where the stronger connection inside the selective neuron pool favors persistent activity and working memory [19]. The memory of the previous stimuli directly causes the hysteresis in the perception. The analysis of nonlinear dynamics on the slow dynamic system indicates that the system could have multiple steady states given proper parameters, for examples, the yellow area in Figs. 5(f) and 6(c), where there are two stable steady states around $\phi=0$. The direct result is that the switching point of perception changes given an increasing of ϕ or decreasing of ϕ in the observation. For the change speed of the external stimuli, the system cannot keep pace with the external stimuli if the external stimuli changes too fast and the hysteresis partly is the consequence of the lag between the external stimuli and the response of the system. The simulation results indicate that a faster change of external stimuli leads to more obvious hysteresis, which is consistent with a recent experiment [23].

One notable thing is the relationship between hysteresis in the perception and bistable perception. For hysteresis in the perception, the perception could change at one point given a sequential changing stimuli, but the perception changes at another point given the same sequential stimuli in a reverse direction. The stimuli change along with time in the experiment as shown in Fig. 1. For bistable perception, the certain stimuli are perceived in a bistable way, alternating between two distinct perceptions. The bistable perception occurs in ambiguous visual displays, ambiguous stimuli in the auditory and tactile domains, and monocular and binocular rivalries. The bistable perception has been extensively studied and the mechanism has been revealed [24,25]. Nevertheless, the stimuli at the two ends of the task of hysteresis in the perception can be clearly classified into one category. Although the stimuli presented in the middle in one trial of the experiment of hysteresis in the perception often are ambiguous, given an ambiguous stimuli for a long time, the subject could perceive the stimuli as one of the two objects presented at the two ends of the task in hysteresis in the perception. Therefore, we investigate the hysteresis but not bistability in perception.

The last thing should be addressed is that our model is not specific to visual hysteresis even we apply it to a visual discrimination task between the man's face and the kneeling girl. The reason is that the input to decision unit is not the direct visual signal from retina or primary visual cortex but is relayed and calculated by higher order cortical structures. For example, in the random dots coherent motion discrimination task, the motion signal is relayed by the middle temporal area to decision unit in the lateral intraparietal area of monkey brain [26]. Therefore, the specialty of the sensory signal is ignored before it is relayed to decision unit in our model. As a consequence, our model cannot discriminate the hysteresis caused by different sensory input, such as visual stimuli, auditory stimuli, olfactory stimuli, and so on. To overcome this shortcoming, the speciality of sensory input must be considered in the future models.

Acknowledgments

This work was supported by the NSFC under Grant No. 60974075 and the Open Funding of the National Key Laboratory of Cognitive Neuroscience and Learning of China. The computation was supported by the HSCC of BNU. The authors are grateful for the helpful comments and suggestions by the anonymous reviewers.

References

[1] D. Williams, G.P.R. Sekuler, Hysteresis in the perception of motion direction as evidence for neural cooperativity, Nature 324 (1986) 253–255.
[2] A. Kleinschmidt, C. Büchel, C. Hutton, K.J. Friston, R.S.J. Frackowiak, The neural structures expressing perceptual hysteresis in visual letter recognition, Neuron 34 (2002) 659–666.
[3] H. Haken, Self-organization of brain function, Scholarpedia 3 (4) (2008) 2555.
[4] H. Haken, Synergetic Computers and Cognition, second ed., Springer, Berlin, 2004.
[5] D.R. Chialvo, V. Apkarian, Modulated noisy biological dynamics: three examples, Journal of Statistical Physics 70 (1) (1993) 375–391.
[6] J.C. Jackson, J.F.C. Windmill1, V.G. Pook, D. Robert, Synchrony through twice-frequency forcing for sensitive and selective auditory processing, Proceedings of National Academy of Science USA 106 (2009) 10177–10182.
[7] H. Haken, Synergetics – An Introduction, Springer, Berlin, 1977.
[8] L.A. Lugiato, P. Mandel, L.M. Narducci, Adiabatic elimination in nonlinear dynamical system, Physical Review A 29 (3) (1984) 1438–1452.
[9] X.-J. Wang, Probabilistic decision-making by slow reverberation in cortical circuits, Neuron 36 (2002) 955–968.
[10] N. Brunel, X. Wang, Effects of neuromodulation in a cortical networks model of object working memory dominated by recurrent inhibition, Journal of Computational Neuroscience 11 (2001) 63–85.
[11] D.J. Amit, N. Brunel, Model of global spontaneous activity and local structured activity during delay periods in the cerebral cortex, Cerebral Cortex 7 (1997) 237–252.
[12] H.C. Tuckwell, Introduction to Theoretical Neurobiology, Cambridge University Press, Cambridge, 1988.
[13] C.E. Jahr, C.F. Stevens, Voltage dependence of NMDA-activated macroscopic conductances predicted by single-channel kinetics, Journal of Neuroscience 10 (1990) 3178–3182.

[14] S. Hestrin, P. Sah, R. Nicoll, Mechanisms generating the time course of dual component excitatory synaptic currents recorded in hippocampal slices, Neuron 5 (1990) 247–253.
[15] N. Spruston, P. Jonas, B. Sakmann, Dendritic glutamate receptor channel in rat hippocampal CA3 and CA1 pyramidal neurons, Journal of Physiology 482 (1995) 325–352.
[16] P.A. Salin, D.A. Prince, Spontaneous GABA receptor mediated inhibitory currents in adult rat somatosensory cortex, Journal of Neurophysiology 75 (1996) 1573–1588.
[17] K.-F. Wong, X.-J. Wang, A recurrent network mechanism of time integration in perceptual decisions, Journal of Neuroscience 26 (4) (2006) 1314–1328.
[18] J. Tegner, A. Compte, X.-J. Wang, The dynamical stability of reverberatory neural circuits, Biological Cybernetics 87 (2002) 471–481.
[19] M. Camperi, X.-J. Wang, A model of visuospatial working memory in prefrontal cortex: recurrent network and cellular bistability, Journal of Computational Neuroscience 5 (2000) 383–405.
[20] S.H. Strogatz, Nonlinear Dynamics And Chaos: With Applications To Physics, Biology, Chemistry, And Engineering, Addison Wesley Publishing, 2001.
[21] Y. Hirai, K. Fukushima, An inference upon the neural network finding binocular correspondence, Biological Cybernetics 31 (1978) 209–217.
[22] D.H. Fender, B. Jules, Extension of Panum's fusional area in binocularly stabilized vision, Journal of Optical Society of America 57 (1967) 819–830.
[23] A. Buckthought, J. Kim, H.R. Wilson, Hysteresis effects in stereopsis and binocular rivalry, Vision Research 48 (2008) 819–830.
[24] G. Gigante, M. Mattia, C. Braun, Paolo Del Giudice. Bistable perception modeled as competing stochastic integrations at two levels, PLoS Computational Biology 5 (7) (2009) e1000430.
[25] H.R. Wilson, Computational evidence for a rivalry hierarchy in vision, Proceedings of National Academy of Science 100 (24) (2004) 14499–14503.
[26] J.D. Roitman, M.N. Shadlen, Response of neurons in the lateral intraparietal area during a combined visual discrimination reaction time task, Nature Neuroscience 22 (21) (2002) 9475–9489.

Hongzhi You is a Ph.D. candidate in Department of Systems Science in Beijing Normal University. His research interests include neural mechanism of perceptual decision making, working memory.

Yan Meng is a Master student in Department of Systems Science in Beijing Normal University, China. Her current research interest is the neuron network of decision making with reference criteria and the dynamics of neural computation.

Di Huan is now in pursuit for M.Sc. degree in Department of Systems Science, Beijing Normal University. His research is related to neuron network modeling and neuronal oscillation.

Da-Hui Wang received Ph.D in Systems Theory from Beijing Normal University in 2002. He is an associate professor at Department of Systems Science. He works on computational neuroscience, especially, the nonlinear dynamics of neural system, dynamics underlying oscillation, working memory, and decision making.